

One- And Two-Dimensional Models For A Linear MHD Generator Channel Design

Author(s): C. A. Borghi, A. Massarini, G. Mazzanti, and P. L. Ribani

Session Name: Generators B

SEAM: 28 (1990)

SEAM EDX URL: <https://edx.netl.doe.gov/dataset/seam-28>

EDX Paper ID: 1429

ONE- AND TWO-DIMENSIONAL MODELS FOR A LINEAR MHD GENERATOR CHANNEL DESIGN

C.A. Borghi, A. Massarini, G. Mazzanti, and P.L. Ribani

Istituto di Elettrotecnica, University of Bologna,
Viale Risorgimento 2, 40136 Bologna, Italy

ABSTRACT

Mathematical models for the design of the linear channel of an MHD generator, are described. By means of a quasi-one-dimensional optimization model the main design parameters of the channel, are calculated. The local phenomena effects are analyzed through a steady state two-dimensional model. This model is based on the description both of the fluid dynamic and of the electrodynamic in the plane containing the channel axis and normal to the magnetic induction. The transients caused by variations of the loading and by faults, are studied by means of a time dependent quasi-one-dimensional model.

NOMENCLATURE

A	channel cross section
B	module of the magnetic induction vector
\vec{B}	magnetic induction vector
E	electric field vector
E_x	axial component of the electric field vector
E_y	transversal component of the electric field vector
F	cost functional
g, g'	constraint expressions
h	static enthalpy
\vec{J}	current density vector
J_x	axial component of the current density vector
J_y	transversal component of the current density vector
k	turbulent kinetic energy
p	static pressure
P	wet perimeter of the channel cross section
Pr _t	turbulent Prandtl number
q _w	thermal flux at the wall
t	time
T	static temperature
U	gas velocity in the axial direction
V	gas velocity in the transversal direction
W	vector of the unknown of the optimization problem
x	axial coordinate (coordinate of the axis of the channel)
y	transversal coordinate (coordinate perpendicular to the plain containing B and the axis of the channel)
β	Hall parameter
γ	specific heat ratio
ϵ	turbulence dissipation rate
λ	thermal conductivity
μ	dynamic viscosity (laminar)
μ_t	eddy viscosity
ν	kinematic viscosity
ρ	mass density
σ	electrical conductivity

τ_w	shear stress at the wall
Φ	electric potential

1. INTRODUCTION

The procedure for the design of a linear MHD channel of industrial size, has been one of the main goals of the MHD activities at the Istituto di Elettrotecnica of the University of Bologna during the last years. In order to do this, one- and two-dimensional models have been developed. The aim of the present paper is to describe the mathematical design procedure. Some typical results obtained for the design of an OCMHD generator channel of industrial size, are presented.

The design procedure approach is based on the three following steps:

- definition of the main channel design parameters by means of an optimization model based on a quasi-one-dimensional description of the plasma flow through the channel;
- determination of the operating characteristics of the end regions, of the boundary layer regions, and of the power extraction regions. In order to do this, a two dimensional analysis of the steady state operation can be utilized;
- determination of the electrical, thermal and mechanical stresses during transients and during the occurrence of faults. This can be obtained through a quasi-one-dimensional time dependent analysis.

The mathematical models which allow to perform this scheme, are described in this paper.

The model for the optimization of the channel design, which utilizes a quasi-one-dimensional approximation for the description of the magnetofluid-dynamic process in the channel, is based on a constrained optimization technique¹. The channel design parameters are chosen with the purpose to maximize the electrical power generated by the MHD generator. Physical and technological requirements are considered. Boundary layer and non-uniformity effects are taken into account.

The two-dimensional steady state MHD model must consider both the fluid dynamic and the electrodynamic phenomena in the channel. The fluid dynamic MHD model is based on the two-dimensional steady compressible form of Navier-Stokes conservation equations. The problem is solved in the x-y plane (the x-axis is the channel axis and the y-axis is the axis perpendicular to the plane containing the channel axis and the magnetic field direction). For the solution of the partial differential equations, the Patankar-Spalding SIMPLE (semi-implicit

pressure linked equations) procedure² has been utilized. The electrodynamic two dimensional description is obtained from the Faraday law, the conservation of the electrical charge and the Ohm's law. A partial differential equation system is obtained and solved through a finite difference technique.

For the solution of the quasi-one-dimensional time dependent description a new computational approach has been adopted. The compressible flow equations for a linear channel are considered. The resulting system of hyperbolic partial differential equations is discretized by means of a semi-implicit finite difference method^{3,4}. The stability of the method does not depend on the speed of sound. The pressure gradient in the momentum equation and the velocity divergence in the energy equation are discretized implicitly. The convective and viscous terms of these equations are discretized explicitly. The mass continuity equation is discretized by means of a conservative scheme. Thus stability and physical meaning of the solution are assured.

The proposed scheme has been utilized for the design calculations of a linear channel of industrial size. A thermal power of 230 MW is obtained by a gas fired combustor. A two load diagonal connection is adopted.

2. CHANNEL OPTIMIZATION

In order to define the main design parameters, as channel geometry, electrical configuration, inlet gas pressure and inlet gas velocity, an optimization technique is utilized.

The description of the MHD conversion process in a linear channel is based on a quasi-one-dimensional approximation. Boundary layer effects on the fluid dynamic are taken into account through integral coefficients introduced into the conservation equations of mass, momentum and energy of the gas^{5,6}. The wall effect in the electrodynamic is considered by means of Rosa's G factor⁷. The combustion gas plasma is considered to be in chemical equilibrium. The equation of state is afforded by spline fits of the thermodynamic properties which are obtained through a free energy minimization technique⁸. The microscopic values of the electrical conductivity and the Hall parameter are obtained through the chemical equilibrium composition of the gas and by means of the formulation of Ref. 9.

The constrained optimization technique described in Ref. 1, is utilized. Physical and technological constraints are taken into account by the solution of the problem. The optimization criterium is based on the maximization of the electrical power output¹⁰. By means of a finite element method the expression of the conservation equations are reduced to a set of algebraic equations which have the form of constraints. The optimization problem is:

$$\text{maximize } F(w) \quad (1)$$

$$\text{subject to } \begin{cases} g(w) = 0 \\ g'(w) \leq 0 \end{cases} \quad (2)$$

The cost functional F is the expression of the quantity which has to be maximized. The algebraic equations obtained from the conservation equations, the electrodynamic equations and the constraints given by equalities are expressed by $g(w) = 0$. The constraints expressed by inequalities are given by $g'(w) \leq 0$. The vector w contains the unknowns of the problem. The constrained optimization problem is solved by means of a quasi-Newton method¹¹ in connection with a multiplier method¹². By means of the optimization model described above, the gas dynamic and the electrodynamic quantities along the channel are chosen when maximizing the functional F and when considering the constraints. The

channel geometry and the electrical configuration are also determined.

Table 1. Inputs of the optimization procedure

Mass flow rate	45 kg/s
Thermal power input	230 MW
Fuel:	CH ₄
Oxidant: enriched air	
- preheating temperature	1973 K
- oxygen content	23 %
Seeding: K ₂ CO ₃	
- weight content	2 %
combustion chamber temperature	2950 K
Pick magnetic induction	5 T

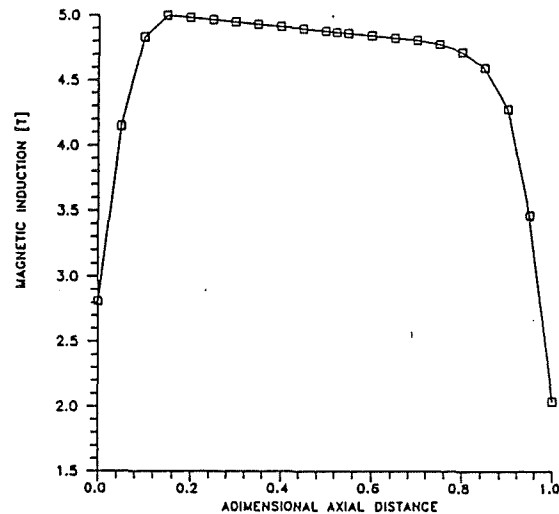


Fig. 1 Magnetic induction distribution along the channel

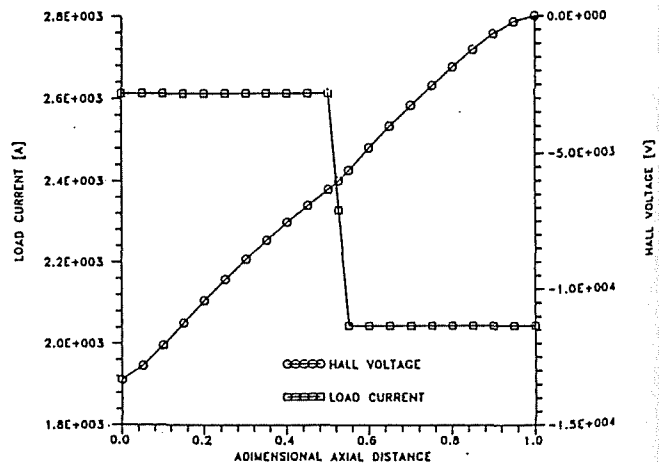


Fig. 2 Distributions of the load current and of the voltage along the channel

This procedure has been utilized for the design parameters of a two load diagonal connected channel. The inputs of the design problem are reported in table 1. The distribution of the magnetic induction in the axial direction is shown in Fig. 1. The flow is assumed to be supersonic. A channel with a square cross section and a constant divergence is taken. The constraints considered are: outlet static pressure greater than 0.75 bar, axial and transversal

component of the electric field respectively lower than 3 kV/m and 4 kV/m, transversal component of the current density lower than 10 kA/m², Mach number greater than 1.01, channel length in the range between 6 and 10 m.

The main results of the optimization procedure are reported in table 2. The distributions of the load current and of the voltage along the channel are shown in Fig. 2. The values of load current refer to the total load current flowing through the channel. Hence in the first part of the plot 2040 A refer to the current flowing through the load connecting the terminal at the channel entrance to the terminal at the channel exit, the remaining 570 A flow through the load connecting the terminal at the entrance to the terminal in the middle of the channel. The stagnation pressure and the gas velocity distributions along the channel are plotted in Fig. 3.

Table 2. Optimized design parameters

Channel volume	1.75 m ³
Active length	6.88 m
Inlet cross section	0.1332 m ²
Outlet cross section	0.3994 m ²
Inlet Mach number	1.45
Inlet gas pressure	1.92 bar
Equipotential angle	58.7 deg.
Electrical Power	31.4 MW
Electrical power density	17.9 MW/m ³
Wall heat losses	7.24 MW

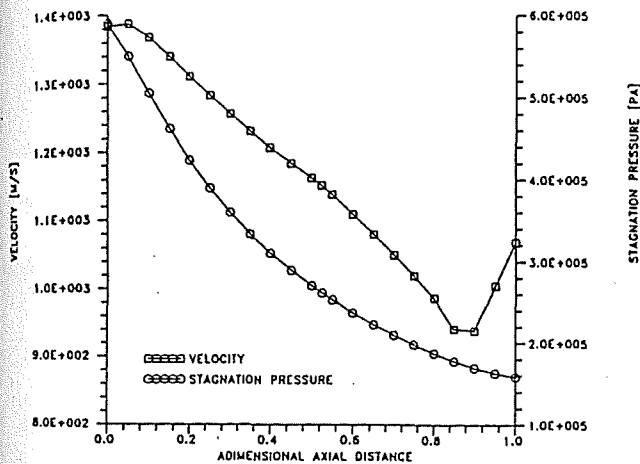


Fig. 3 Stagnation pressure and gas velocity distributions along the channel

3. TWO-DIMENSIONAL CALCULATIONS

The two-dimensional steady state MHD model consists of a fluid dynamic part and of an electrodynamic part, which yield the gasdynamic and electrodynamic properties of the plasma in the x-y plane containing the axis of the MHD duct.

The two-dimensional steady state fluid dynamic MHD model is based on the two-dimensional steady state compressible form of Navier-Stokes conservation equations in the x-y plane. These equations are obtained from the three-dimensional time-dependent conservation equations by means of the Reynolds time-averaging procedure. When assuming for the MHD channel partially parabolic flow conditions^{2,13}, the conservation equations assume the following form¹⁴:

$$\frac{\partial(\rho u)}{\partial x} + \frac{\partial(\rho v)}{\partial y} = 0 \quad (3)$$

$$\rho u \frac{\partial u}{\partial x} + \rho v \frac{\partial u}{\partial y} = -\frac{\partial p}{\partial x} + \frac{\partial}{\partial y} \left[(\mu + \mu_t) \frac{\partial u}{\partial y} \right] + J_y B \quad (4)$$

$$\rho u \frac{\partial v}{\partial x} + \rho v \frac{\partial v}{\partial y} = -\frac{\partial p}{\partial y} + \frac{\partial}{\partial y} \left[2(\mu + \mu_t) \frac{\partial v}{\partial y} \right] - J_x B \quad (5)$$

$$\begin{aligned} \rho u \frac{\partial h}{\partial x} + \rho v \frac{\partial h}{\partial y} = & u \frac{\partial p}{\partial x} + v \frac{\partial p}{\partial y} + \frac{\partial}{\partial y} \left(\lambda \frac{\partial T}{\partial y} + \frac{\mu_t}{Pr_t} \frac{\partial h}{\partial y} \right) + \\ & + (\mu + \mu_t) \left[\left(\frac{\partial u}{\partial y} \right)^2 + 2 \left(\frac{\partial v}{\partial y} \right)^2 \right] + J_x (E_x + v B) + \\ & + J_y (E_y - u B) - \frac{\sigma B^2}{1 + \beta^2} \left[\frac{\mu_t}{\rho} \left(\frac{\partial u}{\partial x} + \frac{\partial v}{\partial y} \right) \right] \end{aligned} \quad (6)$$

The eddy viscosity has been derived by means of the Launder-Jones k-epsilon two equation turbulence model¹⁵. In order to account for the boundary layers, the k-epsilon model version extended to low Reynolds numbers, has been adopted¹⁴. As a result, the equations of the turbulence model assume the following form:

$$\begin{aligned} \rho u \frac{\partial k}{\partial x} + \rho v \frac{\partial k}{\partial y} = & \frac{\partial}{\partial y} \left[\left(\frac{\mu_t}{Pr_k} + \mu \right) \frac{\partial k}{\partial y} \right] + \mu_t \left[2 \left(\frac{\partial v}{\partial y} \right)^2 + \left(\frac{\partial u}{\partial y} \right)^2 \right] - \\ & - \rho \epsilon - 2 \mu_t \left\{ \left[\frac{\partial(k^{1/2})}{\partial x} \right]^2 + \left[\frac{\partial(k^{1/2})}{\partial y} \right]^2 \right\} \end{aligned} \quad (7)$$

$$\begin{aligned} \rho u \frac{\partial \epsilon}{\partial x} + \rho v \frac{\partial \epsilon}{\partial y} = & \frac{\partial}{\partial y} \left[\left(\frac{\mu_t}{Pr_\epsilon} + \mu \right) \frac{\partial \epsilon}{\partial y} \right] + C_1 \mu_t \left[2 \left(\frac{\partial v}{\partial y} \right)^2 + \left(\frac{\partial u}{\partial y} \right)^2 \right] \frac{\epsilon}{k} - \\ & - C_2 \rho \frac{\epsilon^2}{k} + 2 \nu \mu_t \left(\frac{\partial^2 u}{\partial y^2} + \frac{\partial^2 v}{\partial y^2} \right)^2 \end{aligned} \quad (8)$$

where:

$$\mu_t = C_\mu \rho k^2 / \epsilon$$

$$C_\mu = C_{\mu\infty} \exp[-2.5/(1 + Re_t/50)]$$

$$Re_t = k^2 / (\nu \epsilon)$$

$$C_2 = C_{2\infty} [1 - 0.3 \exp(-Re_t^2)]$$

and $Pr_k, Pr_\epsilon, C_1, C_2, C_{\mu\infty}$ are numerical constants.

For the solution of the partial differential equations given by eqs 3-8, the semi-implicit-pressure-linked-equation algorithm (SIMPLE) of Patankar-Spalding^{13,2} has been utilized. According to this algorithm, the computational domain is divided into a number of non-overlapping control volumes. Each control volume surrounds a grid point. The differential equations are integrated inside this volume element. The velocities are calculated at the control volume boundary, the gas pressure and temperature are derived at the grid point. A staggered grid, obtained in this way, avoids solutions without physical meanings, simplifies the form of the discretized equations and improves the rate of convergence.

The convection and diffusion terms in the equations are discretized using the power law scheme², which is very close to the exact solution. This leads to considerable computational time saving. The linear algebraic system derived from the discretization of each equation yields a tridiagonal coefficient matrix, and can be solved with a tri-diagonal matrix algorithm (TDMA).

The two-dimensional steady electrodynamic MHD model is based on Maxwell's equations and on Ohm's law. In the two-dimensional steady state formulation these equations can be written respectively as follows:

$$E_x = -\frac{\partial \phi}{\partial x}, \quad E_y = -\frac{\partial \phi}{\partial y} \quad (9)$$

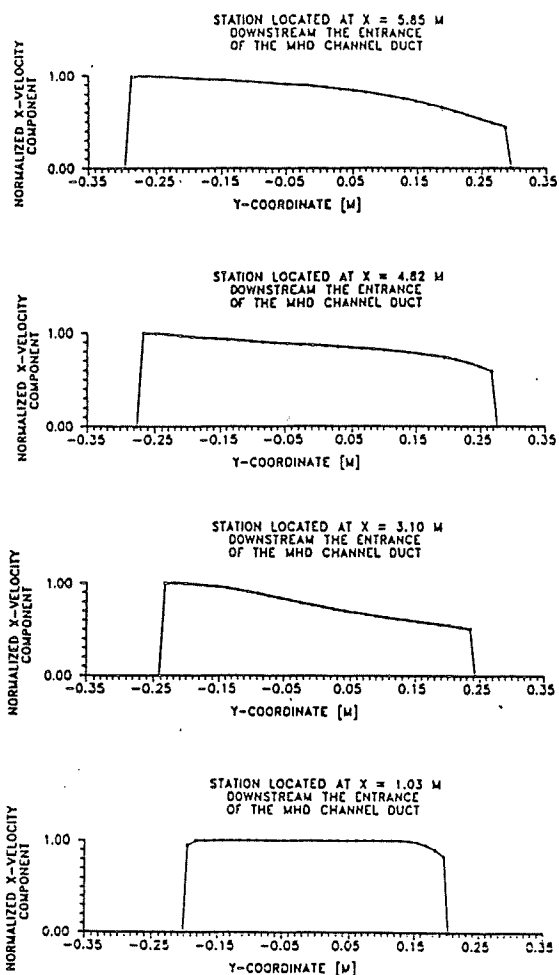


Fig. 4 Adimensional axial velocity profiles along the y-direction at different locations of the channel

$$\frac{\partial J_x}{\partial x} + \frac{\partial J_y}{\partial y} = 0 \quad (10)$$

$$J_x = \frac{\sigma}{1+\beta^2} [(E_x + vB) - \beta(E_y - uB)] \quad (11)$$

$$J_y = \frac{\sigma}{1+\beta^2} [\beta(E_x + vB) + (E_y - uB)] \quad (12)$$

From eq.s 9 through 12 a partial differential equation of the elliptic type in the unknown ϕ (the electric potential), is obtained. This equation has the following expression

$$\begin{aligned} & \frac{\partial^2 \phi}{\partial x^2} + \frac{\partial^2 \phi}{\partial y^2} + \\ & + \frac{\partial}{\partial x} \left[\ln \left(\frac{\sigma}{1+\beta^2} \right) \right] \frac{\partial \phi}{\partial x} + \frac{\partial}{\partial y} \left[\ln \left(\frac{\sigma}{1+\beta^2} \right) \right] \frac{\partial \phi}{\partial y} - \\ & - \beta \left\{ \frac{\partial}{\partial x} \left[\ln \left(\frac{\sigma \beta}{1+\beta^2} \right) \right] \frac{\partial \phi}{\partial y} - \frac{\partial}{\partial y} \left[\ln \left(\frac{\sigma \beta}{1+\beta^2} \right) \right] \frac{\partial \phi}{\partial x} \right\} - \\ & - \frac{1+\beta^2}{\sigma} \left\{ \frac{\partial}{\partial x} \left[\frac{\sigma(\beta u + v)B}{1+\beta^2} \right] - \frac{\partial}{\partial y} \left[\frac{\sigma(u - \beta v)B}{1+\beta^2} \right] \right\} = 0 \quad (13) \end{aligned}$$

The boundary conditions adopted for the solution of eq. 13, are: the potential on the electrodes is constant, the component of current density normal to the insulator surface is equal to zero.

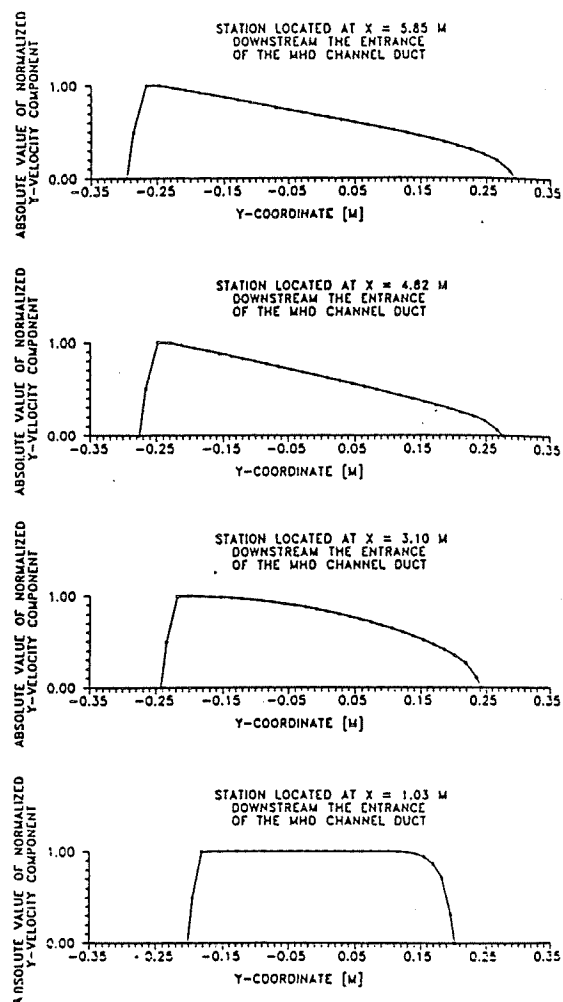


Fig. 5 Adimensional transversal velocity profiles along the y-direction at different locations of the channel

An application of the two dimensional steady state model for the channel of Section 2 is reported. The two dimensional fluid dynamic model is utilized when considering the electrodynamic resulting from a quasi-one-dimensional calculation. In Fig. 4 the adimensional axial velocity profiles along the y-direction at different locations of the channel are shown. Starting with a flat profile at the entrance of the duct, a significant distortion in the profile symmetry arises. This is due to the presence of a positive J_x which causes a significant negative transverse velocity component as Fig. 5 shows. Consequently the axial velocity is higher near the cathode wall than near the anode wall. Moreover the boundary layer at the cathode is much thinner than at the anode. The profile symmetry distortion increases along the channel as long as the axial component of the current density is high. It slightly decreases when J_x becomes smaller than 1000 A/m².

In Fig. 6 the adimensional temperature profiles along the y-coordinate at different locations of the channel are presented. The temperature profile symmetry is also distorted as a consequence of the distortion of the velocity profile.

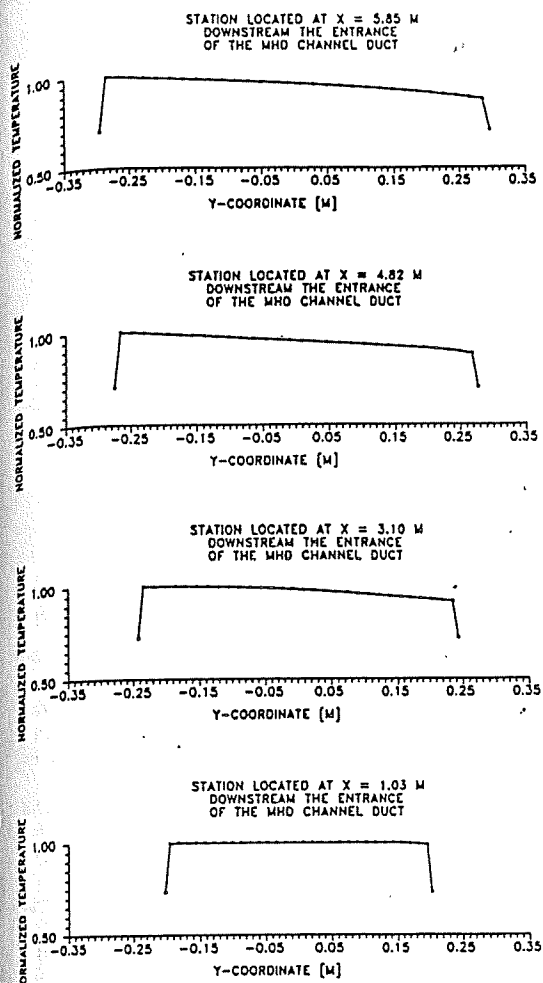


Fig. 6 Adimensional temperature profiles along the y-coordinate at different locations of the channel

4. TRANSIENTS

A quasi-one-dimensional time dependent model of the MHD compressible flow inside the channel has been derived. The conservation equations for mass, momentum and energy assume a partial differential equation form given by

$$\frac{\partial p}{\partial t} + \frac{\partial}{\partial x}(pu) = -\frac{\rho u dA}{A dx} \quad (14)$$

$$\frac{\partial}{\partial t}(\rho u) + \frac{\partial}{\partial x}(\rho u^2) = -\frac{\partial p}{\partial x} - \frac{\rho u^2 + p dA}{A dx} - \tau_w \frac{P}{A} + J \times B \quad (15)$$

$$\begin{aligned} \frac{\partial p}{\partial t} + u \frac{\partial p}{\partial x} = & -\gamma p \frac{\partial u}{\partial x} - p \frac{u dA}{A dx} + \\ & + (\gamma - 1) \left[(\tau_w u - q_w) \frac{P}{A} + J \cdot E - u J \times B \right] \end{aligned} \quad (16)$$

where the energy balance equation (eq. 16) is expressed in terms of the static pressure p . The form of Ohm's law given by eq.s 11 and 12 where the transversal velocity component v is considered to be zero, is utilized. Electrical boundary conditions related to the type of the channel (segmented Faraday or diagonal conducting sidewall) have been considered.

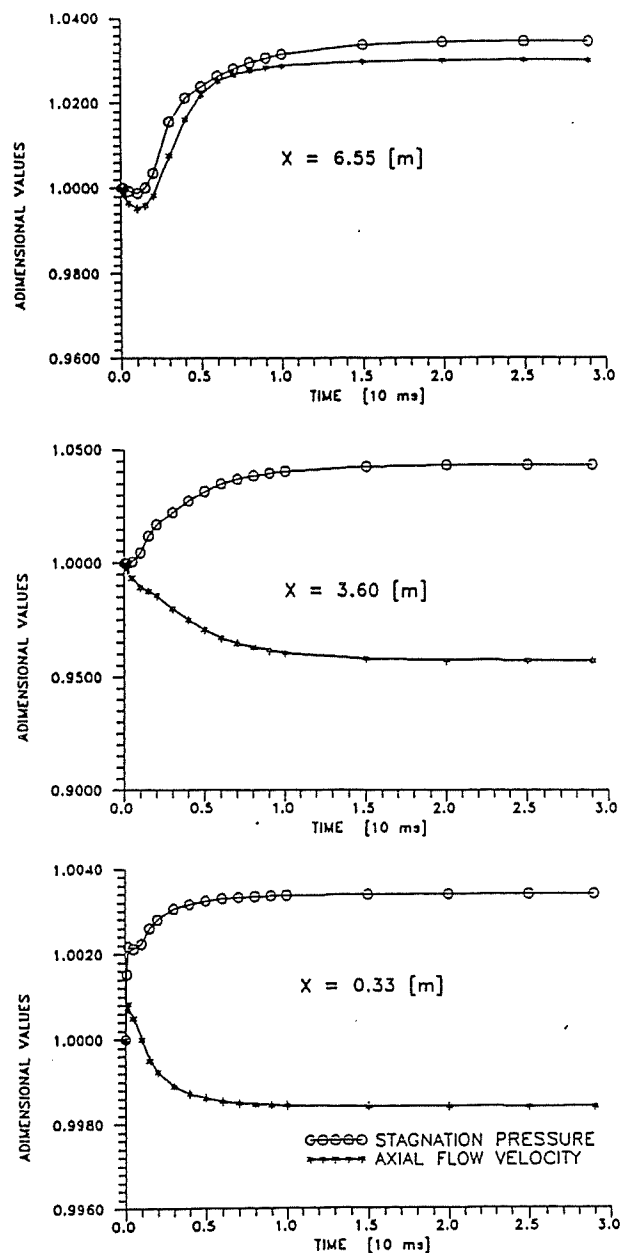


Fig. 7 Time behaviours of the stagnation pressure and of the gas velocity at the entrance region, in the middle of the channel and at its exit

A semi-implicit difference scheme, according to the approach proposed by Casulli^{3,4}, has been applied for the solution of the model. Since the speed of sound represents a singular solution for an explicit method, some terms in the governing equations are discretized implicitly. In order that the numerical method may be unconditionally stable with respect to the speed of sound, the terms $\partial p / \partial x$ in the momentum equation and $\partial u / \partial x$ in eq. 16 must be discretized implicitly. Hence through the semi-implicit discretization of eq.s 14-16, the following results are obtained:

$$\rho_i^{n+1} = \rho_i^n - \frac{\Delta t}{\Delta x} [(\rho u)_i^n - (\rho u)_{i-1}^n] - \Delta t \rho_i^n u_i^n \left(\frac{1}{A} \frac{dA}{dx} \right)_i \quad (17)$$

$$u_i^{n+1} = G_i^n - \frac{1}{\rho_i^n \Delta x} (p_{i-1/2}^{n+1} - p_{i+1/2}^{n+1}) \quad (18)$$

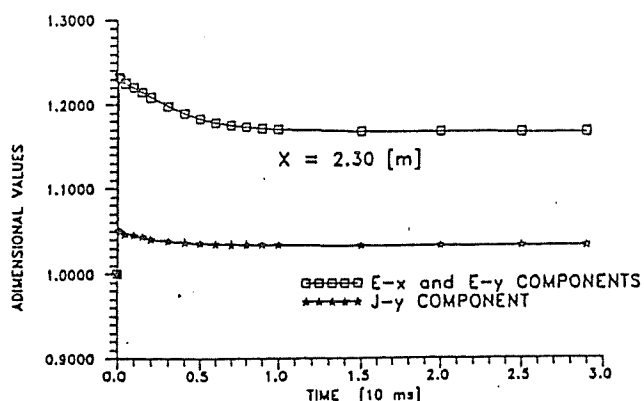


Fig. 8 Time behaviours of the axial and transversal components of the electric field and of the transversal current density at one third of the channel length

$$p_i^{n+1} = H_i^n - \gamma p_i^n \frac{\Delta t}{\Delta x} (u_{i-1/2}^{n+1} - u_{i-1/2}^{n-1}) \quad (19)$$

where the superscript n , $n+1$ refer to time discretization and the subscript i , $i+1/2$, $i-1/2$ refer to space discretization. G and H are nonlinear functions. In this case the following expressions have been derived for them:

$$G_i^n = u_i^n - \frac{\Delta t}{\Delta x} u_i^n (u_i^n - u_{i-1}^n) +$$

$$\frac{\Delta t}{\rho_i^n} \left[(J \times B)_i^n - \tau_w \left(\frac{P}{A} \right)_i \right] - \Delta t \frac{p_i^n}{\rho_i^n} \left(\frac{1}{A} \frac{dA}{dx} \right)_i \quad (20)$$

$$H_i^n = p_i^n - \frac{\Delta t}{\Delta x} u_i^n (p_i^n - p_{i-1}^n) + \Delta t \left\{ (\gamma - 1) \left[(u_i^n \tau_w^{n+1} - q_w^{n+1}) \left(\frac{P}{A} \right)_i - u_i^n (J \times B)_i^n + (J \cdot E)_i^n \right] - p_i^n u_i^n \left(\frac{1}{A} \frac{dA}{dx} \right)_i \right\} \quad (21)$$

A first order accuracy is obtained. The method is stable when satisfying the following condition:

$$\Delta t \leq \frac{\Delta x}{|u|} \quad (22)$$

which depends on the velocity of the plasma only.

The transient following a change in the loading of the MHD generator of Section 2, is considered. The unsteady situation is caused by halving the two load currents (following a decreased electrical power request) at the time $t = 0$. The time behaviours of the stagnation pressure and of the gas velocity at the entrance region, in the middle of the channel and at its exit are shown in Fig. 7. The adimensional values plotted in all graphs refer to the values assumed at $t = 0$. A relaxation time of the order of 10 ms is observed. The velocity decreases at the entrance and in the middle of the channel whereas it increases at the exit. The stagnation pressure increases in all positions. This is a consequence of the reduction of the request of electrical power. The time behaviours of the axial and transversal components of the electric field and of the transversal current density at one third of the channel length are shown in Fig. 8. After the transient the absolute values of E_x , of E_y and of J_y result to be increased. Therefore the electrical stress can become too large.

CONCLUSIONS

The procedure for the design calculations of an MHD linear channel has been presented. Three main steps in the design have been distinguished and the mathematical models related to them have been described. An optimization model based on a quasi-one-dimensional approximation is utilized for the definition of the main design parameters. In order to analyze the channel operation near the walls and in the power extraction regions a two-dimensional model has been developed. This model can study the electrodynamic and the fluid dynamic operation in the plane containing the channel axis and normal to the magnetic induction vector. For the third step a quasi-one-dimensional time dependent model has been developed. The numerical solution of it is done through the Casulli algorithm^{3,4}. This three step procedure has been utilized for the design of a 230 MWt gas fired channel.

REFERENCES

1. Borghi, C.A., Negrini, F., and P.L. Ribani, *Constrained Optimal Control Problem for MHD Flows*, to appear on *Magnetohydrodynamics: an International Journal*.
2. Patankar, S.V., *Numerical Heat Transfer and Fluid Flow*, Hemisphere Publishing Company, 1980.
3. Casulli, V. and Greenspan, D., *Pressure Methods for the Numerical Solution of Transient, Compressible Fluid Flows*, International Journal for Numerical Methods in Fluids, Vol. 4, pp. 1001-1012, 1984.
4. Casulli, V., *Eulerian-Lagrangian Methods for the Navier-Stokes Equations at High Reynolds Number*, International Journal for Numerical Methods in Fluids, Vol. 8, pp. 1349-1360, 1988.
5. Borghi, C.A., Negrini, F., and Ribani, P.L., *Mathematical Modeling for the Channel Design of a Combustion Plasma MHD Generator*, 2nd International Workshop on Fossil Fuel Fired MHD Retrofit of Existing Power Stations, pp. 185-194, Bologna (Italy), 1990.
6. Biturkin, V.A., Lyubimov, G.A., Medin, S.A., and Ponomarev, V.M., *Engineering Methods of Flow Calculation for an MHD Generator Channel*, Teplofizika Vysokikh Temperatur, Vol. 12, pp. 817-826, Moscow, 1973.
7. Rosa, R.J., *Boundary Layer Voltage Loss Comparison*, Proc. 19th Symp. EAM, pp. 5.3.1-6, Tullahoma (Tenn.), 1981.
8. Zelesnik, F.J., and Gordon, S., *Calculation of Complex Chemical Equilibria*, Ind. Eng. Chem., Vol. 60, n. 6, pp. 27-57, 1968.
9. Demetriades, S.T., and Argyropoulos, G.S., *Ohm's Law in Multicomponent Nonisothermal Plasmas with Temperature and Pressure Gradients*, The Physics of Fluids, Vol. 9, pp. 2136-2149, 1966.
10. Borghi, C.A., and Ribani, P.L., *Criteria for the Optimization of MHD Generator Channel Flows*, Proc. 10th Int. Conference on MHD Electrical Power Generation, Vol. 2, pp. X.152-156, Tiruchirapalli (India), 1989.
11. Dennis, J.E., Jr., and Schnabel, B., *Numerical Methods for Unconstrained Optimization and Nonlinear Equations*, Prentice-Hall, Englewood Cliff (New Jersey), 1983.
12. Bertsekas, D.P., *Constrained Optimization and Lagrange Multiplier Method*, Academic Press, 1982.
13. Patankar S.V., Spalding D.B., *A Calculation Procedure for Heat, Mass and Momentum Transfer in three-dimensional Parabolic Flows*, International Journal on Heat and Mass Transfer, Vol. 15, pp. 1787-1806, 1972.
14. Ishikawa M., Umoto J., *New Approach to Calculation of 3D Flow in MHD Generators*, Proc. 22th Symp. EAM, pp. 2.8.1-18, Starkville (Mississippi), 1983.

15. Launder B.E., Spalding D.B., *The Numerical Computation of Turbulent Flows*, Computer Methods in Applied Mechanics and Engineering, Vol.3, pp. 269-289, 1972

16. Jones W.P., Launder B.E., *The Prediction of Laminarization with a Two-Equation Model of Turbulence*, International Journal on Heat and Mass Transfer, Vol.15, pp. 301-314, 1972

re
e
al
l-
al
in
el
on
is
ic
nd
rd
del
ne
re
ed

ned
on

low,

for
fluid
s in

the
tum-
s in

ritical
asma
ossil
ions,

and
Flow
fizica
scow,

rison,
enn.),

complex
6, pp.

's Law
Tem-
ics of

Opti-
.. 10th
ration,
39
ethods
ations
83
grange

cedure
ree-di-
nal on
3, 1972
ition of
EAM